DEVELOPMENT OF A LASER-BASED SYSTEM FOR TESTING CONSTRUCTION AGGREGATE

Hyoungkwan Kim (hyoungkwan@mail.utexas.edu)
Graduate Research Assistant, University of Texas at Austin, TX, 78712, USA

Carl T. Haas (haas@mail.utexas.edu)
Associate Professor, University of Texas at Austin, Austin, TX, 78712, USA

Alan F. Rauch (arauch@mail.utexas.edu)
Assistant Professor, University of Texas at Austin, Austin, TX, 78712, USA

Craig Browne (cbrowne@geosyntec.com)
Staff Engineer, GeoSyntec Consultants, Boxborough, MA, 01719, USA

Abstract: A Laser-based Aggregate Scanning System (LASS) was developed at the University of Texas at Austin for rapid characterization of various properties of construction aggregates. For the determination of shape and size parameters, the “virtual proportional caliper” and “virtual sieve” concepts are introduced, where 3D particle data are rotated about different axes to find elongation and flatness ratios, and the smallest mesh opening size through which a particle can pass. This paper also proposes a group texture based quality control method using wavelet analysis. This method is expected to provide fast group characterization of aggregates during production, enabling real time quality monitoring.

Keywords: aggregate, automation, group texture analysis, laser profiling, LASS, virtual proportional caliper, virtual sieve, wavelet analysis.

1. INTRODUCTION

The importance of using aggregate with specific characteristics is gaining increased recognition in the construction industry. To ensure that high quality aggregate products are used, efforts are being made to test more frequently. However, some common methods for aggregate testing like ASTM C136 (Standard Test Method for Sieve Analysis of Fine and Coarse Aggregates) and ASTM D4791 (Standard Test Method for Flat Particles, Elongated Particles, or Flat and Elongated Particles in Coarse Aggregate) are time consuming and labor intensive. Moreover, for prompt adjustment of the aggregate production process, fast aggregate characterization methods are necessary.

A prototype laser scanner was developed for the purpose of characterizing aggregates in a fast, accurate, and reliable way. Using laser profiling, this system is able to capture three-dimensional (3D) data on aggregate particles. The “virtual proportional caliper” and “virtual sieve” concepts are used to simulate the manual processes of measuring the shape and the gradation of aggregate particles. In these “virtual” methods, each particle’s 3D data are incrementally rotated about different axes to calculate elongation and flatness ratios, and the smallest mesh opening size through which the particle can pass [1]. This paper also proposes a group texture based quality control method using wavelet analysis. This method is expected to provide condensed critical information on aggregates as they are produced, enabling real time quality controls.

2. LASER-BASED AGGREGATE SCANNING SYSTEM (LASS)

The "Laser-based Aggregate Scanning System" (LASS) consists of a laser line scanner, a linear motion slide, and a personal computer (Figure 1). The laser scanner, which is mounted on the linear motion slide, passes over an aggregate sample, scanning it with a vertical laser plane. This system is designed to provide maximum flexibility for the study of different scanner velocities and spread patterns while repeatedly scanning the same field of aggregates scattered randomly on a table. The 3D data obtained in this way are transformed into 8-bit grayscale digital images, where grayscale pixel values represent the height of each data point. A comprehensive explanation of the LASS can be found in [2].

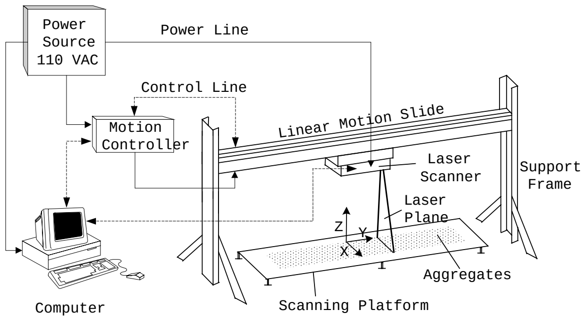

Figure 1. The Laser-based Aggregate Scanning System (LASS).

3. 3D IMAGE SEGMENTATION

An aggregate sample that is randomly scattered on the platform is likely to have particles that touch each other. Accordingly, the particles should be separated in the captured image by a particle segmentation algorithm for accurate assessment of each particle. For this purpose, a method for segmenting particle images acquired from laser profiling was developed using a Canny edge detector [3] and a watershed transform [4]. This method combines particle shape and height gradient information. For example, while a distance map [5] used for the watershed transform provides particle shape information, it does not show gradients of the image. On the other hand, while Canny edges are entirely relevant to the image gradients, they are not strongly related to particle shape. It is possible to obtain better segmentation results by combining these two non-redundant bits of information.

The segmentation algorithm is as follows:

1. A particle image acquired from laser profiling is thresholded into a binary image.
2. Rough particle outlines are drawn on the binary image using Canny edges detected with rigorous threshold values.
3. The binary image is transformed into a distance map.
4. Regional minima [4] of the distance map are identified with a varying search window approach, where the number of neighboring pixels being compared with the pixel of interest is determined proportionally to the height value of the pixel.
5. The identified regional minima are given unique labels, and they expand through a binary dilation process [5] until they meet other regions, including the original background regions.
6. When the growing regions meet other regions, the borders between them are set as watersheds.
7. The validity of the watersheds is checked by comparison with Canny edges detected with liberal threshold values. That is, if the watersheds do not have corresponding Canny edges, the regions separated by them are merged.
8. Finally, to compensate for some possible data loss from the self-occlusion problem [5], voids in each particle region are filled with the horizontally closest pixel height values in the region.

4. VIRTUAL PROPORTIONAL CALIPER AND VIRTUAL SIEVE

It is assumed that the aggregates are oriented in the most stable position when spread out on the platform. The largest height value of the particle is then the thickness or the shortest primary dimension. Once the shortest dimension is obtained, calculating the intermediate and longest dimensions becomes a two-dimensional problem [1]. That is, disregarding the height data, the particle image is projected onto a two-dimensional (2D) plane. An algorithm is then used to incrementally rotate the particle to find the smallest rectangle that circumscribes the projected image. This process can be thought of as a “virtual proportional caliper”. The length and the width of the rectangle then become the particle’s longest and intermediate dimensions, respectively. In case the particle does not rest flat, the three primary dimensions are sorted by magnitude to determine the true longest, intermediate, and shortest dimensions. Finally, the elongation and flatness ratios are calculated for each particle [1].

Next, the “virtual sieve” is performed, where each particle’s projected image along the longest dimension is incrementally rotated to find the smallest circumscribing square. That square’s dimension becomes the smallest mesh size through which the particle can pass. However, in many cases, a particle that cannot pass a certain mesh size in this “virtual sieve” actually can pass through that opening size in a slightly different orientation. To correct for this effect, a reduction factor of 0.85, which was determined from examining various oversized particles, is used to calculate the actual mesh opening that the particle can pass through.

To verify the performance of the LASS in determining particle shape parameters, 200 particles, ranging from 7 to 26 mm in their longest dimension, were manually measured in order to compare with the results from the LASS. To get samples that have a range of particle colors and surface textures, aggregates were procured from four different quarries in the United States. From each source, fifty particles were randomly selected making a total of 200 particles. To measure the three primary dimensions of each particle, a vernier caliper (0.025 mm accuracy) was used. The manual measurement of the 200 particles required approximately four hours with the aid of a computer spreadsheet program to calculate the elongation and flatness ratios. For the volume measurement, each particle was immersed in a water-filled graduated cylinder (100 mm^3 divisions) where the change in water level corresponded to the particle volume. For the volume measurement, approximately seven hours were required. After the manual measurements were completed, the particles were scattered on the LASS platform, scanned, and analyzed. The resolutions for X, Y, and Z directions (see Figure 1) were 0.3 mm, 0.3 mm, and 0.5 mm respectively. It took 70 seconds to scan the 200 particles, and 40 seconds to calculate elongation and flatness ratios.

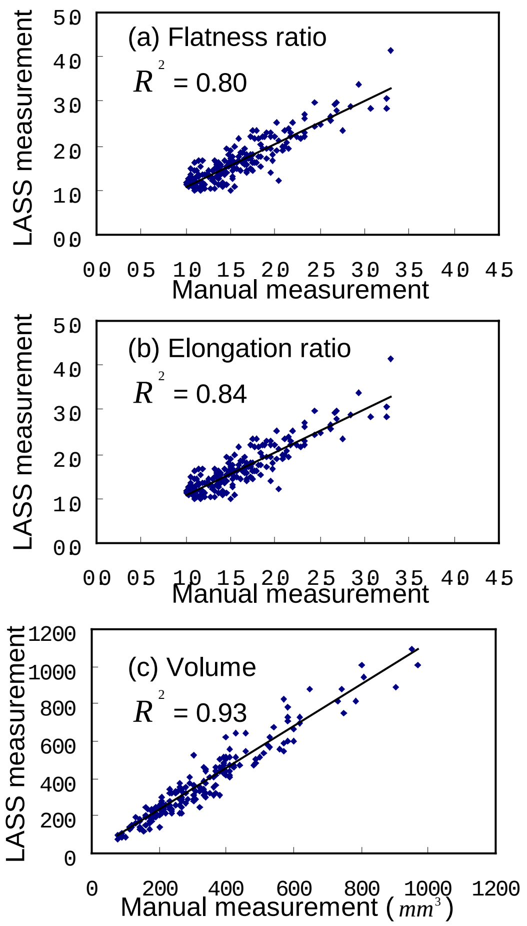

Figure 2. Comparison between the manual and LASS measurement: (a) Flatness ratio; (b) Elongation ratio; (c) Volume.

Figure 2 shows the results of the correlation analysis conducted to see how the manual measurements compared to the LASS results. All three show that there are strong correlations between the manual and LASS measurements.

In preparation for evaluating the performance of the LASS in determining particle size parameters, eight benchmark aggregate samples of different grain size distributions and shapes were assembled. The eight samples were comprised of the following four different materials, two samples per material: river gravel, traprock, granite, quartzite. The samples, each approximately 1 kg, contained particles ranging in size from 2.36 mm (#8 sieve) to 19 mm (3/4 inch sieve). After the aggregate samples were manually spread on the platform, the data were captured and analyzed to obtain the grain size distribution. It took approximately 8 minutes to scan one aggregate sample and calculate volume and equivalent mesh size. Figure 3 shows the comparison results where the sieve data are represented as dots indicating their discrete nature. Due to space limitations, only one particle size distribution is presented. As seen from Figure 3, results from the manual sieve analysis and the LASS compare very well.

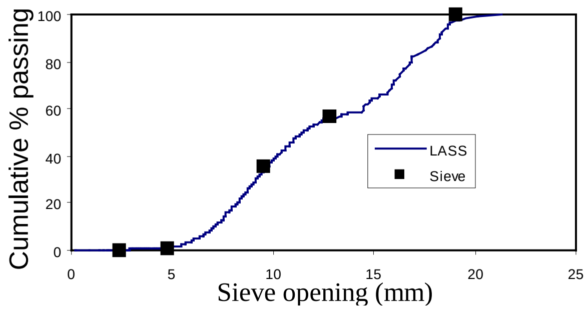

Figure 3. Comparison of a size distribution result between the manual and LASS measurements.

5. GROUP TEXTURE BASED QUALITY CONTROL

The “virtual proportional caliper” and the “virtual sieve” methods rely on measurements of each particle’s shape and size parameters. By implementing these methods in various areas such as laboratories, large construction sites, and so on, construction material quality is expected to improve. However, if the application is primarily concerned with variations in the product rather than complete characterization, a much faster method can be used. For example, in aggregate production plants, the gradation of aggregates is monitored based on variations in the percent passing a specified sieve size [6]. Thus, by monitoring variances, plant operators can know whether the production process needs to be adjusted. In addition, the method of extracting the variance information is likely to facilitate faster analysis because it does not require the complete particle characterization process of measuring all particles after segmenting them.

Wavelet analysis is one method that can compress a vast amount of LASS data to a degree that product variance information can be easily extracted. It decomposes a signal into a group of linear combinations with each combination having different resolutions. This transform is conducted by using a finite length of a basis function called a “mother wavelet”. The “mother wavelet” is compared with the signal to be analyzed by changing its length (dilation) and location (translation) in order to find where and how much each dilated and translated version of it coincides with the signal. The dilation and translation mechanism of the “mother wavelet” enables not only production of localized information in space and frequency domains, but also effective representation of the signal. The following paragraphs reviews 1D and 2D wavelet analysis and is based on the work presented in [7], [8], and [9]. Building upon these formulations, a texture-based method is proposed for controlling quality during aggregate production.

5.1 Wavelet Analysis

Particle images obtained from the LASS go through a wavelet analysis to obtain a better information format. Wavelet analysis can best be explained with its intrinsic characteristic of Multi Resolution Analysis (MRA). Figure 4 shows how to decompose a signal into a group of linear combinations. V_0, V_1, and V_2 are vector spaces such that V_0 is a subspace of V_1, and V_1 is a subspace of V_2. W_0 and W_1 are “difference” vector spaces between V_0 and V_1, and V_1 and V_2, respectively. These relationships can be expressed as

$$V_0 \oplus W_0 = V_1 \qquad (1)$$

$$V_1 \oplus W_1 = V_2 \qquad (2)$$

where $\oplus$ stands for vector addition.

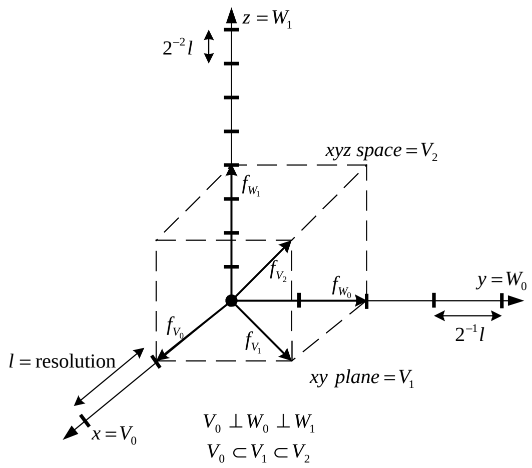

Figure 4. Decomposition of a signal $f(t)$ using wavelet analysis.

Figure 4 also shows that the vector spaces V_0, W_0, and W_1 are mutually orthogonal. If Figure 4 shows all the vector spaces available, the most accurate approximation of a signal $f(t)$ can be obtained by projecting it on V_2, which is f_{V_2}. Likewise, if more approximations are needed for the signal, f_{V_1} and f_{V_0}, projections on V_1 and V_0 respectively, would minimize the information loss. This implies that the signal can be represented with various levels of approximations, minimizing possible information loss on each. That is, depending on the degree of accuracy required, various levels of the difference vector (f_{W_0}, f_{W_1}, and so on) can be added to the initial approximation f_{V_0} in order to represent the signal. As an example, the signal f_{V_2} can be expressed as

$$f_{V_2} = f_{V_0} + f_{W_0} + f_{W_1} \qquad (3)$$

Expansion of the vector spaces can generalize Equation (3) into

$$f(t) = f_{V_0} + \sum_{j=0}^{\infty} f_{W_k} \qquad (4)$$

Since f_{V_0} and f_{W_k} can also be represented as a linear combination of basis functions, Equation (4) can be expressed as

$$f(t) = \sum_{k=-\infty}^{\infty} c_{0,k}\varphi_{0,k}(t) + \sum_{j=0}^{\infty}\sum_{k=-\infty}^{\infty} d_{j,k}\psi_{j,k}(t) \qquad (5)$$

where $\varphi_{0,k}(t)$ and $c_{0,k}$ are basis functions and their corresponding coefficients for f_{V_0}, respectively, and $\psi_{j,k}(t)$ and $d_{j,k}$ are basis functions and their corresponding coefficients for f_{W_k}, respectively. Here, the basis function $\varphi_{0,k}(t)$ for the initial approximation of a signal is called the “scaling function”, and the basis function $\psi_{j,k}(t)$ for the difference vectors are called the “wavelet”. Note that as the level of difference vector space goes up, better resolution is obtained in Figure 4. This implies that as j goes up, the length over which the wavelet $\psi_{j,k}(t)$ exists is reduced. This aspect of wavelet analysis called MRA enables an efficient representation of a signal in the sense that high frequency parts of the signal are represented with better resolution than low frequency parts.

By expanding the area of j to negative infinity, Equation (5) turns into

$$f(t) = \sum_{j=-\infty}^{\infty}\sum_{k=-\infty}^{\infty} d_{j,k}\psi_{j,k}(t) \qquad (6)$$

Therefore, if wavelets $\psi_{j,k}(t)$ are orthonormal to each other, wavelet coefficients $d_{j,k}$ are expressed as

$$d_{j,k} = < f(t), \psi_{j,k}(t) > = \int_{-\infty}^{\infty} f(t)\psi_{j,k}(t)dt \qquad (7)$$

where <*x*, *y*> means inner product of *x* and *y*. Equation (7) is called the wavelet transform.

Wavelets are obtained by scaling and translating the so-called “mother wavelet” in the following manner [7].

$$\psi_{j,k}(t) = \frac{1}{\sqrt{j}}\psi\left(\frac{t-k}{j}\right),\ j > 0,\ j,k \in R \qquad (8)$$

where ψ is the “mother wavelet”, *j* and *k* are scale and translation coefficients, respectively. $1/\sqrt{j}$ in

Equation (8) is for making the norm of $\psi_{j,k}(t)$ into 1 [7]. Note that *j* is the inverse concept of frequency.

The mother wavelet is a compactly supported (finite length) function that has the following properties [7]:

$$\int_{-\infty}^{\infty} \psi(t)dt = 0 \tag{9}$$

$$\|\psi\| = 1 \tag{10}$$

where $\|x\|$ is norm of x, i.e. $< x, x >$. When 2 is used as the scale *j*, as in most cases, Equation (8) is as follows [7]:

$$\psi_{j,k}(t) = 2^{j/2}\psi\left(2^j t - k\right),\ \ j,k \in R \tag{11}$$

These compactly supported wavelets enable wavelet coefficients $d_{j,k}$ to drop off rapidly allowing for efficient representation of the signal. In conclusion, wavelet analysis transforms and comparts a 1D signal into a 2D time(space)–frequency domain showing where and how much the dilated and translated versions of the mother wavelet correlate with the signal.

5.2 2D wavelet analysis

2D wavelet analysis begins by defining 2D basis functions by multiplication of scaling function $\varphi(x)$ and $\varphi(y)$. Then, from the orthonormal characteristic of the 2D basis functions [7], a signal $f(x,y)$ (2D image) can be represented as

$$f_1(x,y) = \sum_{i=-\infty}^{\infty}\sum_{j=-\infty}^{\infty} a_1(i,j)\varphi(2x-i)\varphi(2y-j) \tag{12}$$

on V_1. Since $\sum_{i=-\infty}^{\infty} a_1(i,j)\varphi(2x-i)$ in Equation (12) is a 1D signal and can be represented as a sum of the approximation on V_0 and the difference vector on W_0, it becomes

$$\sum_{n=-\infty}^{\infty} a_{0,j}(n)\varphi(x-n) + \sum_{n=-\infty}^{\infty} b_{0,j}(n)\psi(x-n) \tag{13}$$

Putting Equation (13) in Equation (12),

$$f_1(x,y) = \sum_{j=-\infty}^{\infty}\sum_{n=-\infty}^{\infty} a_{0,j}(n)\varphi(x-n)\varphi(2y-j) + \sum_{j=-\infty}^{\infty}\sum_{n=-\infty}^{\infty} b_{0,j}(n)\psi(x-n)\varphi(2y-j) \tag{14}$$

Likewise, if $\sum_{j=-\infty}^{\infty} a_{0,j}(n)\varphi(2y-j)$ and $\sum_{n=-\infty}^{\infty} b_{0,j}(n)\varphi(2y-j)$ in Equation (14) are decomposed into their approximations and difference vectors,

$$f_1(x,y) = \sum_{i=-\infty}^{\infty}\sum_{j=-\infty}^{\infty} c_0(i,j)\varphi(x-i)\varphi(y-j) + \sum_{i=-\infty}^{\infty}\sum_{j=-\infty}^{\infty} d_{0,0}(i,j)\varphi(x-i)\psi(y-j) + \sum_{i=-\infty}^{\infty}\sum_{j=-\infty}^{\infty} d_{0,1}(i,j)\psi(x-i)\varphi(y-j) + \sum_{i=-\infty}^{\infty}\sum_{j=-\infty}^{\infty} d_{0,2}(i,j)\psi(x-i)\psi(y-j) \tag{15}$$

Thus, by adding an infinite number of difference vectors to the initial approximation, $f(x,y)$ is obtained as follows:

$$f(x,y) = \sum_{j=-\infty}^{\infty}\sum_{k=-\infty}^{\infty} c_0(j,k)\varphi(x-j)\varphi(y-k) + \sum_{i=0}^{\infty}\sum_{j=-\infty}^{\infty}\sum_{k=-\infty}^{\infty} d_{i,0}(j,k)\varphi(2^{-i}x-j)\psi(2^{-i}y-k) + \sum_{i=0}^{\infty}\sum_{j=-\infty}^{\infty}\sum_{k=-\infty}^{\infty} d_{i,1}(j,k)\psi(2^{-i}x-j)\varphi(2^{-i}y-k) + \sum_{i=0}^{\infty}\sum_{j=-\infty}^{\infty}\sum_{k=-\infty}^{\infty} d_{i,2}(j,k)\psi(2^{-i}x-j)\psi(2^{-i}y-k) \tag{16}$$

Taking the lower limit of *i* to negative infinity in Equation (16) and using the orthonormal characteristic of 2D basis functions, wavelet coefficients can be obtained as follows:

$$d_{i,j,k,l} =< f(x,y), W_{i,j,k,l}(x,y) >$$
$$= \int_{-\infty}^{\infty} f(x,y)W_{i,j,k,l}(x,y)dxdy,\ \ i,j,k \in Z,\ l \in [0,2]$$

where
$$W_{i,j,k,0} = \varphi(2^{-i}x-j)\psi(2^{-i}y-k)$$
$$W_{i,j,k,1} = \psi(2^{-i}x-j)\varphi(2^{-i}y-k)$$
$$W_{i,j,k,2} = \psi(2^{-i}x-j)\psi(2^{-i}y-k) \tag{17}$$

Figure 5 shows a three-level decomposition of an

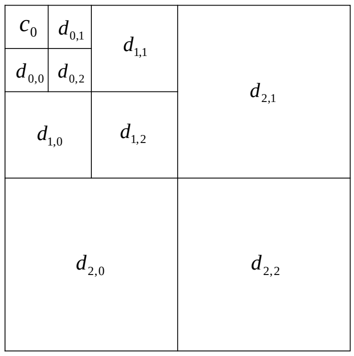

Figure 5. A three-level decomposition of a signal $f(x,y)$ using wavelet analysis.

image. While c_0 is simply an approximation of the image, $d_{i,j}$ are detail (difference) information at each different resolution level *i*. Here, $d_{i,0}$, $d_{i,1}$, and $d_{i,2}$ show vertical, horizontal, and diagonal edge information, respectively. In practical discrete wavelet transform calculations, a signal is passed through a high pass filter and a low pass filter, with values that are associated with each wavelet system, and down sampled to produce wavelet coefficients. This is because the wavelet transform is essentially a convolution operation [7].

5.3 Texture Based Quality Control Method

In the machine vision field, texture can be defined as a combination of texture elements and the relations between each element. Aggregate particles can correspond to texture elements with certain special relationships with each other. If a group of construction aggregates are scanned into an image, this image can be considered as a texture. One method to quantify texture uses edge information in the image. For example, the number of edge pixels in a certain size area can be used for texture description. However, texture description is highly scale dependent [5]. For example, edges detected with high resolution would be ignored if low resolution was used. This is where the value of wavelet analysis comes in. As discussed previously, wavelet analysis provides vertical, horizontal, and diagonal edge information on various scales. Therefore, using this information, it is possible to quantify the texture of an aggregate image effectively and objectively. Then, by comparing this quantified information between in-spec and out-of-spec aggregate images, any aggregate group with out-of-spec gradation can be detected as unacceptable.

The following features are proposed:

- Standard Deviation of $c_0(j,k)$
- $\sum_{j=-\infty}^{\infty}\sum_{k=-\infty}^{\infty}\sum_{l=0}^{2}\left|d_{i,l}(j,k)\right|$, $i \in [0,4]$
- Standard Deviation of $d_{i,l}(j,k)$, $i \in [0,4]$

The eleven features, which are obtained through five levels of wavelet decomposition of laser-based aggregate images, are expected to well differentiate a group aggregate with out-of-spec gradation, in conjunction with a classifier such as artificial neural networks. For basis functions, Daubechies' wavelets [8], which are known to work well with natural images, will be used.

6. CONCLUSION

The Laser-based Aggregate Scanning System (LASS) was applied to the characterization of shape and size parameters of aggregates. For the determination of shape parameters, the "virtual proportional caliper" method was used, where individual particle data were rotated along their shortest dimension direction to find elongation and flatness ratios. For gradation analysis, the "virtual sieve" method was used, where the particle data were rotated along the longest dimension direction to calculate its equivalent mesh opening size. To save aggregate sample preparation time, a method for segmenting particle images acquired from laser profiling was also developed based on fusion of the Canny edge detector and a watershed transform. In the verification test, the LASS measurements of the flatness ratio, elongation ratio, volume, and particle size distributions all showed very strong correlations with the manual measurements, demonstrating that the LASS is a powerful tool for particle characterization.

The LASS is also expected to provide group texture based aggregate information that can be used for quality control in aggregate production plants. The proposed wavelet-based features extracted from the aggregate image acquired from laser profiling are extremely promising in the sense that they represent the aggregate in an effective way, and they can be obtained rapidly. This ability will enable aggregate producers to monitor various aspects of product quality during their production, so that immediate process adjustments can be made to ensure better quality products.

ACKNOWLEDGMENTS

The authors wish to thank the International Center for Aggregates Research (ICAR) for providing the funding that made this study possible.

REFERENCES

[1] H. Kim, C. Browne, A. F. Rauch, and C. T. Haas. "A Prototype Laser Scanner for Characterizing Size and Shape Parameters in Aggregates." *Proc., 9th Annual Symposium, ICAR,* Austin, Texas, April, 2001.

[2] H. Kim, C. Browne, A. F. Rauch, and C. T. Haas. "Innovative System for Scanning Construction Aggregates using Laser Profiling." *Proc., 17th International Symposium on Automation and Robotics in Construction,* Taipei, September, 2000.

[3] J. Canny. "A computational approach to edge detection." *IEEE transactions on pattern analysis and machine intelligence*, 8(6), 679-698, 1986.

[4] S. Beucher, and C. Lantuejoul. "Use of watersheds in contour detection." *Proc., Int. Workshop on Image Processing, Real-Time Edge and MotionDetection/Estimation,* Rennes, France, 1979.

[5] M. Sonka, V. Hlavac, and R. Boyle. *Image Processing, Analysis, and Machine Vision*, PWS Publishing, 1999.

[6] R. D. Barksdale. *The Aggregate Handbook*, National Stone Association, Washington, D.C., 1993.

[7] S. Mallat. *A Wavelet Tour of Signal Processing, Second Edition*, Academic Press, San Diego, California, 1999.

[8] I. Daubechies. *Ten Lectures on Wavelets,* CBMS series, SIAM, Philadelphia, Pennsylvania, 1992.

[9] R. M. Rao, and A. S. Bopardikar. *Wavelet Transforms*, Addison Wesley Longman, Inc., Reading, Massachusetts, 1998.